An Examination of the Systematic Properties of Source Lists for WFPC2 and ACS Derived from SExtractor

Michael A. Wolfe and Stefano Casertano

ABSTRACT

The study of the systematic properties of source lists that have been generated via a reduction pipeline within the Hubble Legacy Archive can disclose how satisfactorily the source lists are constructed. If the source lists are created in a robust and consistent manner then the investigation of the systematic properties of source lists can be done by removing astrometric and rotational offsets to reveal any detector characteristics that might arise. This can be explored through the various residuals that remain after subtraction of the aforementioned offsets. Furthermore, prior to the removal of the rotational offsets numerous plots can give qualitative information as to whether there is a large or small angle offset that is to be removed. This information can be inferred from the distribution of data points and the slopes correlated with these distributions. Moreover, after the removal of these offsets and looking at the data from an overall view point instead of on an individual basis, information can be derived that point to charge transfer efficiency, throughput, sensitivity, and quantum efficiency losses. Also, it is possible to detect any problems with calibration files if the source of the anomaly is not tied to any detector characteristics. The derivation of this information can only be the aftermath of a consistent and appropriate derivation of each individual source list.

1. Introduction

The examination of systematic properties is an important step in producing a product that is robust in all aspects when that product is repeatedly demanded by a group of people. Therefore, this examination is essential in the production of source lists that are generated through the Hubble Legacy Archive (HLA) from Hubble Space Telescope (HST) photometric observations[1]. The exploration of the systematic properties of source lists can also expose any errors or non-optimal parameter values that go into source list generation. The source lists are created from a pipeline that uses DAOphot and Source Extractor (SExtractor; Bertin & Arnouts 1996) to calculate

[1]Based on observations made with the NASA/ESA Hubble Space Telescope, and obtained from the Hubble Legacy Archive, which is a collaboration between the Space Telescope Science Institute (STScI/NASA), the Space Telescope European Coordinating Facility (ST-ECF/ESA) and the Canadian Astronomy Data Centre (CADC/NRC/CSA).

astrometry and fluxes. Note that the version of DAOphot used is an IRAF[2] implementation, not Peter Stetson's original program (Stetson 1987). The fluxes derived from DAOphot and SExtractor are subsequently used to generate magnitudes in the AB magnitude system (Oke & Gunn 1983). In order to perform a systematic examination pertaining to HLA source lists we assembled a catalogue of observations that cover an overlapping field of view (FOV), are separated in time, and done in several different filters. From these source lists we have matched, via right ascension and declination, objects found in the two source lists, hereafter referred to as paired source lists. Paired source lists refer to two source lists where one is designated the reference source list and the other is the compared source list. Note, however, that if there is more than one compared source list (and this is generally the case) with regards to a reference source list then paired source lists only refer to the reference source list and only one compared source list. No source lists that are designated as compared source lists are paired.

After astrometric offsets have been derived and removed, matches between the paired source lists are determined. After the matches have been ascertained rotations (if any and however small) have been removed as well. We will step through each modification and show via plots and tabular information the knowledge that can be inferred from the current data sets. The paired source lists employed in this analysis were observed with Wide Field Planetary Camera 2 (WFPC2; 73 paired source lists) and Advanced Camera for Surveys (ACS; 8 paired source lists) using mainly the F606W and F814W filters. The source lists will be compared and analyzed after the astrometric offsets have been removed and with and without rotation. Furthermore, outliers have been identified and analyzed to determine if the cause is due to DAOphot or SExtractor or if there are anomalies in the exposures themselves. In order to facilitate the examination of the systematic properties of HLA source lists several Interactive Data Language (IDL) programs were written and adopted to analyze paired source lists. See Wolfe & Casertano 2011a for an analysis showing that the outliers are from the single and final drizzled images and not from the HLA pipeline.

2. The Data

The pipeline that generates the source lists outputs a text file that has a header and numerous columns. The header contains information regarding observational parameters and numerous quantitative and qualitative values produced during the derivation of source lists by SExtractor, *i.e.,* data quality flags, aperture correction, processing dates, whether the charge transfer efficiency (CTE) correction was done, and the Modified Julian Date (MJD) used in calculating the CTE. The main body of the source list has columns that pertain to astrometry, identification numbers, photometry (aperture and CTE corrected magnitudes), sky values, fluxes, concentration indexes, data quality flags, isophotal fluxes, Kron aperture (Kron 1980), and CTE values (note that the

[2]IRAF is distributed by the National Optical Astronomy Observatory, which is operated by Associations of Universities for Research in Astronomy, Inc., under cooperative agreement with the National Science Foundation.

source lists produced by SExtractor contain 140 columns). The range of the data covers roughly 8 years, from: January 23, 1996 through April 18, 2004. There were numerous filters used and these are: F300W, F336W, F410M, F450W, F467M, F547M, F555W, F606W, F675W, F702W, and F814W. However, the most frequent filters used in this analysis are F606W and F814W.

Throughout the rest of this document source lists will be designated first by proposal number and secondly by the visit identification, e.g., 08048_02 and 05941_04. When the source lists are compared the one with the most recent date of observation is employed as a reference, while all other source lists, which of course, possess the same field of view and filter, are considered to be the comparison source lists. The source lists used in this analysis were required to have the same FOV with a leeway of $10''$ because pointings in each of the exposures used to create the source lists will not be exactly the same. This is a consequence of using exposures that come from various proposals and times. As a final requirement only paired source lists with more than 50 matches are used in the analysis, as this number is adequate for a robust measure of offsets, angles, and slopes.

3. Part I: Individual Source List Comparison Results

3.1. Astrometric Offset

The astrometric offset is determined using the idl software match_sex_cat.pro, which reads in the source lists and then finds offsets by taking the right ascensions and declinations contained within the reference source list and subtracting every entry found in the comparison source list. The differences are put into differential right ascension and differential declination bins and the bin containing the most counts is then used as the offset that is then subtracted from the right ascensions and declinations found in the reference source list. Before relating the information provided by analyzing numerous right ascension and declination plots it will be important to explain what the four plots are in Figures 1, 3, 5, and 7. The first figure (upper left) has a plot of differential right ascension vs. right ascension and the second figure (upper right) is a plot of differential declination vs. declination. The bottom two plots are differential declination vs. right ascension (left) and differential right ascension vs. declination (right). Figures 1, 3, 5, and 7 show that the astrometric offset has been removed leaving only the residuals that have the rotational offset.

3.2. With Rotation

In this section we will compare and analyze paired source lists that still have a rotational offset in right ascension and declination. At this stage we can determine if there is any residual offset that has not been taken out of the right ascension and declination. We find in the top left and right of Figure 1, which is a comparison between 08048_02 and 05941_04, shows distinct non-random distributions that signify a substantial rotation between the two source lists. In the

bottom left and right plots of Figure 1, it is shown that there is a correlation between the slopes and that they are negatives of each other. This behavior proves that there is a significant rotation between the two source lists being compared. Demonstration of rotations between paired source lists can also be discerned from vector plots. A vector plot is a plot in which pairs of points are drawn as vectors. If there is a significant rotation between paired source lists then when the vectors are drawn, all or a majority of the vectors will distribute themselves in a circular fashion. This is because the rotation between the two source lists offsets the right ascension and declination in the same direction. The vectors will increase in size from the center of the FOV as well and is a result of the arc lengths ($s = r\theta$) increasing as vectors are displaced from the center of the FOV. This behavior manifests itself as a rotational vector field, which is shown in Figure 2. The size of the vectors and the rotational distribution of the vectors depends on the magnitude of the rotational offset. Therefore, it is clear from the vector field in Figure 2 (comparison between 08048_02 and 05941_04) that there is a significant rotational offset that has to be removed. In contrast, the comparison between 08048_02 and 07274_04, as shown in Figure 3, depicts a random distribution in the top two plots. Moreover, these random distributions display slopes that are both positive and the bottom two plots show small slopes that have opposite signs, but this represents a modest rotational offset. Inspection of Figure 4 confirms that there is essentially no rotational offset as the vectors point in random directions as opposed to the rotation displayed by the vectors in Figure 2.

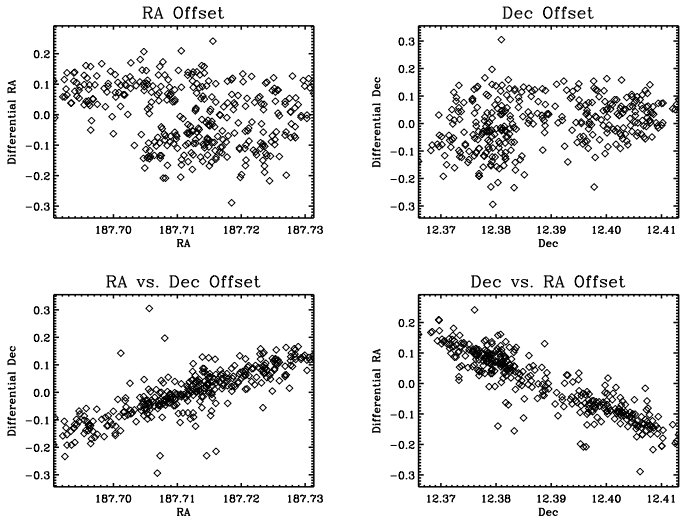

Fig. 1.— The two upper plots show that there is a distinct non-random distribution. The two lower panels show slopes that are negatives of each other and this reveals that there is a significant rotation. The abscissas are in decimal degrees and the ordinates are in arcsec. The source lists compared are 08048_02 and 05941_04.

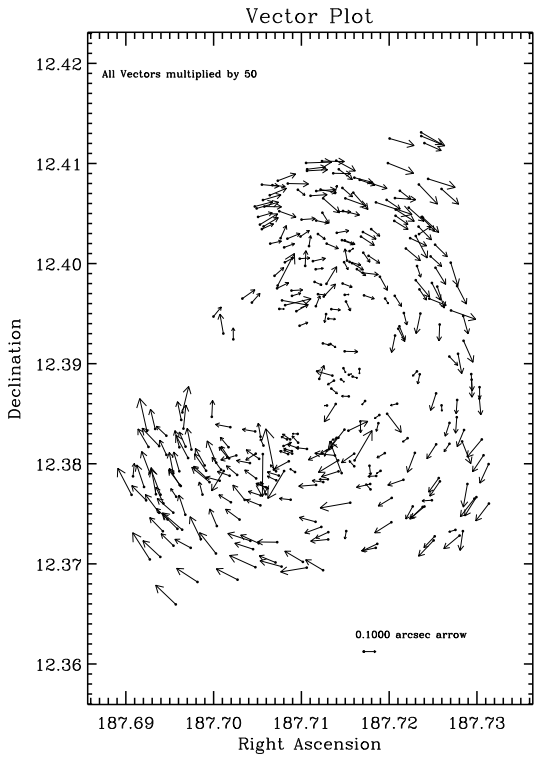

Fig. 2.— This vector field plot shows that there is a considerable rotation to be removed from the source lists being compared. The amount of rotational offset can be found Table 1. The abscissas and ordinates are in decimal degrees. The source lists compared are 08048_02 and 05941_04. Note that all vectors are multiplied by 50 to enhance the vector field.

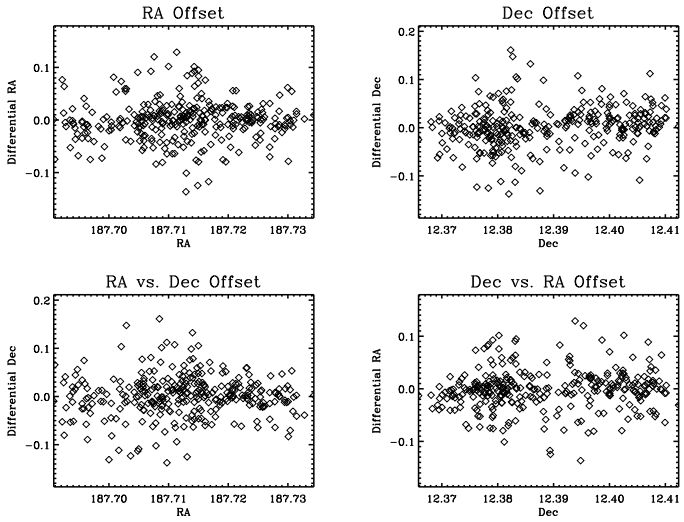

Fig. 3.— The two upper plots show that there is a random distribution in the data around zero, however, there does appear to be slopes in each distribution. The two lower panels show limited slopes that are negatives of each other, which represents a modest rotation. The slopes in the top and bottom plots are used to measure different parameters (see Section 3.3) associated with the paired source lists and therefore will have different values. The abscissas are in decimal degrees and the ordinates are in arcsec. The source lists compared are 08048_02 and 07274_04.

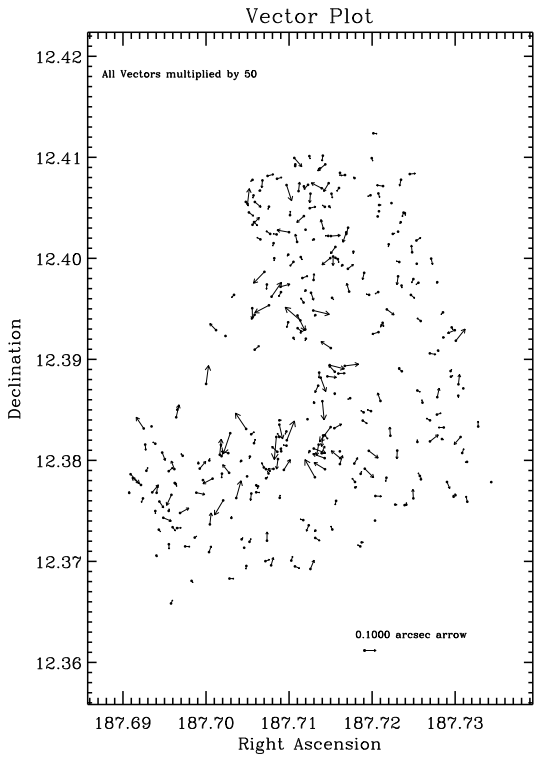

Fig. 4.— This vector field plot does not reveal a rotation between the two source lists being compared. The abscissas and ordinates are in decimal degrees. The source lists being compared are 08048_02 and 07274_04. Note that all vectors are multiplied by 50 to enhance the vector field.

3.3. Without Rotation

In this section we continue our analysis and comparison of source lists, however, in these cases the rotational offsets has been removed. In order to remove the rotational offsets the right ascension and declination of both source lists are mapped to each other. A least squares fit is used to map from one source list to another and the three angles that are derived give the best fit for the transformation. Additionally, in this transformation no small angle approximations were undertaken. The rotation was then removed from the second source list (not the reference source list). Table 1 has the astrometric and rotational offsets that were removed from all of the paired source lists and the RMSs of the differential right ascension and differential declination after the astrometric and rotational offsets have been removed. Table 1 has columns of the instruments used to generate the source lists, data sets compared, dates of the observations, Δright ascension (differential right ascension) and standard deviations, Δdeclination (differential declination) and standard deviations, rotational offsets, Δright ascension and Δdeclination RMSs and the filter

employed in the observations. Now that both offsets have been removed any residuals should be related to the detector characteristics. Since we have source lists that span several years we can determine how the detector changes with time, if at all.

Before proceeding to make comparisons of the various figures it is important to describe what potential detector characteristics can be determined from the residuals after removing astrometric and rotational offsets. For starters, if the two top plots (differential right ascension vs right ascension and differential declination vs declination, left and right top plots, respectively) have slopes that are of the same sign then this is an indication of a change in plate scale. This change in plate scale can be calculated to within an order of magnitude by obtaining the average of both slopes. Moreover, if the slopes are of opposite signs of each other then the detector characteristic that can be approximated is a type of skew. The skew in this case represents different plate scales for right ascension and declination and is derived by calculating the difference in the slopes. For the bottom two plots (differential declination vs right ascension and differential right ascension vs declination, left and right bottom plots, respectively) if the slopes are the same then this is a measure of another type of skew, but in this case it is a measure of how much deviation there is from perpendicularity between the axes within each individual source list. This particular skew is estimated by computing the average of both slopes. If, however, the slopes are of opposite sign then this means that there still remains a rotational offset.

To begin, compare the two upper plots of Figures 1 and 5 and notice that the non-random distribution in Figure 1 has been replaced with a random distribution about zero. Furthermore, note that in the two lower plots in Figure 5 the slopes have disappeared and plots now show a random distribution about zero. Both of these pieces of evidence confirm that rotation has been mitigated. Additionally, comparison of Figures 2 and 6 reveal also that the rotation has indeed been removed as the rotational distribution of the vectors seen in Figure 2 has been replaced with a random distribution of vectors in Figure 6. Investigation of Figure 3 illuminates that there are slopes associated with the two upper plots as well as small but opposite slopes manifested in the two lower plots. Contrasting Figure 3 with Figure 7 shows that the rotational offset has been removed because the slopes in the bottom plots are approximately the same and have the same signs. Inspection of the top plots of Figures 3 and 7 show essentially no difference after the removal of rotational offsets, which implies that the slopes exhibited are possibly due to changing detector characteristics as the observations span about 6 years for the source lists 08048_02 and 05941_04 and approximately 3 years for the paired source lists 08048_02 and 07274_04. Figures 4 and 8 both show no rotational vectors but do display random vectors, which implies that there is no apparent rotational offset between the paired source lists 08048_02 and 07274_04. However, in Figure 3 small opposite signed slopes appear in the bottom two plots. This means that the vector plots along with Figure 3's bottom plots should be used in conjunction to verify a rotational offset.

The change in plate scale and a measurement of both types of skews can be found in Table 2. Note that in the plots the slopes have units of arcsecs/degree ($''/\circ$) and the resultant plate scale changes and skews have been divided by $3600''$. Consequently the units now divide out ($\circ/\circ$)

and only a number is left. The columns of Table 2 are: data sets compared, Δplate scale, skew (plate scale), and skew (perpendicularity between axis). By comparing to the slopes found from other paired source lists it has been determined that the slope values found in the two paired source lists analyzed in this document are representative of the entire set of paired source lists. Furthermore, the small values presented in Table 2 imply that the plate scale of WFPC2 has changed insignificantly over time and that both skews have little consequence after astrometric and rotational offsets have been expunged. The axis skew should be small as the data was taken at a low value for the declination. As the declination increases the right ascension arcs become smaller and is related to the declination through the $\cos(\delta)$ factor used in calculating the right ascension arcs. When the declination increases and the right ascension arcs decrease this imparts a non-perpendicularity between the two axes within the individual source lists. Additionally, the FOV of the observations will show a miniscule effect of non-perpendicularity as the ranges for right ascension and declination are small. Mathematical derivations for Δplate scale, plate scale skew, and rotation can be found in the Appendix.

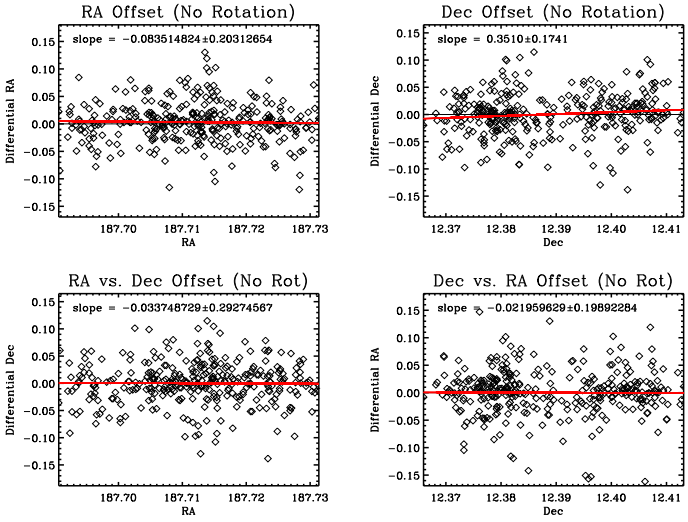

Fig. 5.— The two upper plots show that the distinct non-random distribution has been removed. The two lower panels show a random distribution with slopes of the same sign, which clearly indicates that the rotation has been removed. The red line is a least-square polynomial fit to the data. The abscissas are in decimal degrees and the ordinates are in arcsec. The source lists compared are 08048_02 and 05941_04.

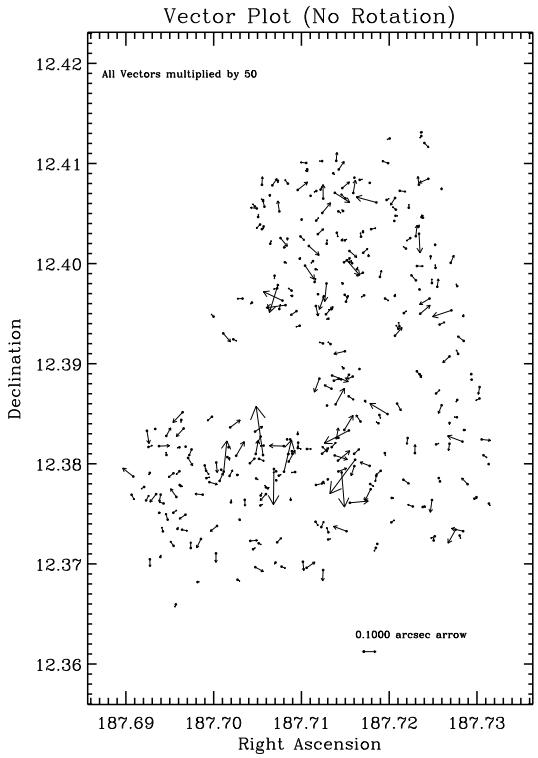

Fig. 6.— This vector field plot shows that the rotation has been removed from the source lists being compared. The abscissas and ordinates are in decimal degrees. The source lists compared are 08048_02 and 05941_04. Note that all vectors are multiplied by 50 enhance the vector field.

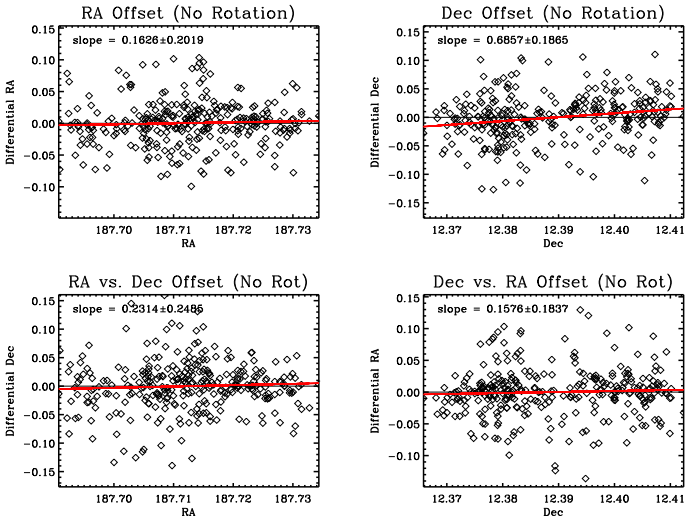

Fig. 7.— The upper left plot reveals positive slopes in both plots that still remain after astrometric and rotational offsets have been removed. The two lower panels show a random distribution that have slopes of the same sign, which clearly indicates that the rotation has been removed. The red line is a least-square polynomial fit to the data. The abscissas are in decimal degrees and the ordinates are in arcsec. The source lists compared are 08048_02 and 07274_04.

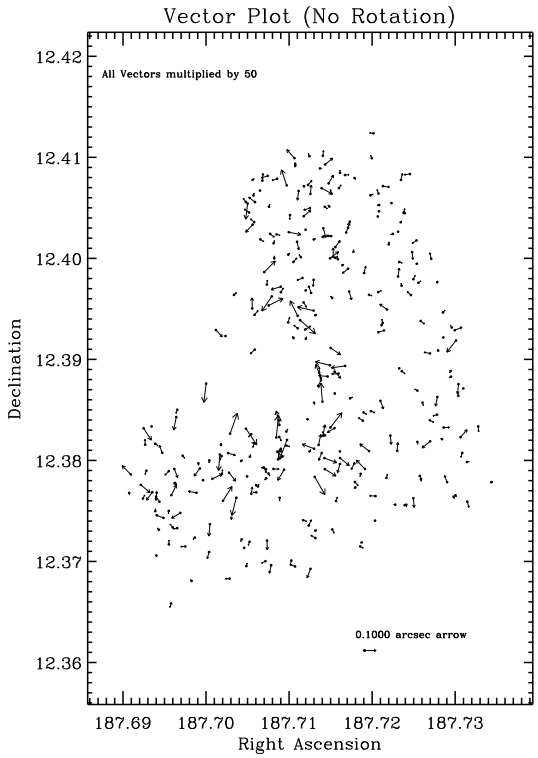

Fig. 8.— This vector field plot reveals relatively no change after the small rotation between the two source lists has been removed. The abscissas and ordinates are in decimal degrees. The source lists being compared are 08048_02 and 07274_04. Note that all vectors are multiplied by 50 to enhance the vector field.

Table 1: Offsets Between Source Lists and RMS

Instr	Data Comp	Data Ref	Date Comp	Date Ref	ΔRA″	ΔRA″ Stddev	ΔDec″	ΔDec″ Stddev	ΔRot°	ΔRot° Error	ΔRA RMS″	ΔDec RMS″	Filter
acs	9438_01	9438_13	2003.0385	2004.087	0.0095	0.0127	0.0058	0.0114	-0.0008	0.0028	0.0121	0.01	f814w
acs	9438_01	9438_03	2003.0385	2003.057	-0.0037	0.0355	0.0016	0.0359	-0.0003	0.0092	0.054	0.0491	f814w
acs	9438_02	9438_13	2003.0409	2004.087	-0.009	0.0135	0.0086	0.012	0.0004	0.0028	0.0125	0.0106	f814w
acs	9438_02	9438_03	2003.0409	2003.057	-0.016	0.0405	-0.0036	0.0306	0.0024	0.0093	0.0563	0.0489	f814w
acs	9438_03	9438_13	2003.057	2004.087	0.0108	0.0354	0.0059	0.0379	-0.0015	0.0095	0.0524	0.0434	f814w
acs	9438_04	9438_05	2003.0517	2004.0793	-0.0105	0.0103	0.0076	0.0088	-0.0004	0.003	0.0097	0.0083	f555w
acs	9811_01	9811_05	2004.2129	2004.2961	-0.0105	0.0114	0.0134	0.0129	-0.0006	0.003	0.011	0.0111	f606w
acs	9811_04	9811_05	2004.2951	2004.2961	0.0152	0.0139	0.0175	0.0142	-0.0029	0.0029	0.013	0.0131	f606w
wfpc2	5477_0d	8048_02	1995.0879	2001.8732	0.0443	0.1164	-0.6762	0.096	0.1369	0.0057	0.0511	0.0469	f814w
wfpc2	5941_04	8048_02	1995.8881	2001.8732	0.11	0.1038	-0.7549	0.0878	0.1178	0.0056	0.0456	0.0532	f814w
wfpc2	7274_04	8048_02	1998.1485	2001.8732	-0.2464	0.0445	-0.3305	0.0446	-0.0014	0.0058	0.0437	0.0451	f814w
wfpc2	8059_dd	8059_dh	2000.6166	2000.6214	-0.0163	0.0786	0.006	0.0236	-0.0002	0.0037	0.1321	0.0383	f606w
wfpc2	8059_df	8059_dh	2000.6159	2000.6166	-0.0144	0.0666	-0.0028	0.0208	-0.0001	0.0022	0.1062	0.0347	f606w
wfpc2	6129_04	6129_05	1996.0479	1996.0644	-0.0605	0.1223	-0.0122	0.1137	0.0086	0.0049	0.1493	0.1364	f814w
wfpc2	6251_3u	7274_23	1995.5132	1999.4537	0.0213	0.1179	-0.0415	0.126	0.141	0.0087	0.1051	0.0905	f814w
wfpc2	6251_3v	7274_23	1995.5134	1999.4537	-0.0097	0.1221	-0.0117	0.1081	0.1402	0.0068	0.0644	0.0522	f814w
wfpc2	6251_3w	8090_if	1995.5138	1999.4533	0.0048	0.122	-0.0055	0.0956	0.1363	0.0073	0.0511	0.0401	f606w
wfpc2	6251_3x	8090_if	1995.514	1999.4533	0.0141	0.1201	-0.0109	0.0971	0.1413	0.0073	0.0357	0.0358	f606w
wfpc2	6251_3z	7274_22	1995.5037	1999.4565	-0.0033	0.1291	-0.1028	0.1131	0.1358	0.0086	0.0938	0.0817	f814w
wfpc2	6251_40	7274_22	1995.5039	1999.4565	-0.0395	0.1258	0.0371	0.1062	0.143	0.0091	0.075	0.0608	f814w
wfpc2	6251_41	7274_22	1995.5041	1999.4565	0.0173	0.1158	0.0108	0.1145	0.1416	0.0089	0.0673	0.0807	f814w
wfpc2	6254_aa	6254_ac	1996.1622	1996.1625	3.495	0.0397	-1.1964	0.0322	0.0053	0.0131	0.039	0.0346	f814w
wfpc2	6254_ab	6254_ad	1996.1623	1996.1627	-0.4826	0.0337	0.0187	0.0377	-0.0026	0.0125	0.036	0.0379	f606w
wfpc2	6802_7b	6802_7e	1997.42	1997.4377	0.0471	0.0495	-0.3341	0.0608	0.0067	0.012	0.0816	0.0769	f814w
wfpc2	6802_7c	7909_jk	1997.4202	1998.3711	-0.0206	0.0484	0.0281	0.048	-0.0041	0.0123	0.0483	0.0479	f606w
wfpc2	6938_06	7629_05	1998.4949	1999.4241	0.0036	0.0401	-0.0018	0.0304	-0.0035	0.0029	0.0434	0.03	f814w
wfpc2	7202_ry	7202_s1	1997.7348	1997.7354	-0.0765	0.1382	0.002	0.069	-0.0063	0.0032	0.4324	0.1511	f450w
wfpc2	7202_rz	7202_s0	1997.735	1997.7352	0.0315	0.0716	0.0172	0.0347	0.0028	0.0102	0.1732	0.0761	f814w
wfpc2	7505_22	7505_26	1998.1072	1999.0995	-0.0064	0.0285	-0.0144	0.0294	-0.0027	0.0122	0.0287	0.0293	f814w
wfpc2	7505_23	7505_26	1998.1289	1999.0995	-0.004	0.0235	-0.0333	0.0286	-0.006	0.0121	0.0261	0.0281	f814w
wfpc2	7505_24	7505_26	1998.1694	1999.0995	-0.0591	0.0259	-0.0976	0.024	0.0009	0.012	0.0261	0.0238	f814w
wfpc2	7505_25	7505_26	1998.2165	1999.0995	-0.0045	0.0243	0.0053	0.0282	-0.005	0.0122	0.0245	0.0279	f814w
wfpc2	7505_51	7505_57	1999.0813	2000.0981	0.0187	0.0395	-0.0058	0.0335	-0.0014	0.0105	0.0367	0.0352	f814w
wfpc2	7505_52	7505_57	1999.0976	2000.0981	-0.0055	0.0423	-0.001	0.041	0.0022	0.0107	0.042	0.0415	f814w
wfpc2	7505_53	7505_57	1999.1173	2000.0981	-0.0045	0.0477	-0.0015	0.0364	0.0025	0.0105	0.0474	0.0364	f814w
wfpc2	7505_54	7505_57	1999.1374	2000.0981	-0.0214	0.0415	-0.0106	0.0307	-0.0022	0.0104	0.0417	0.0306	f814w
wfpc2	7505_55	7505_57	1999.1556	2000.0981	0.0041	0.0372	-0.0057	0.0288	0.0073	0.0105	0.034	0.0283	f814w
wfpc2	7505_56	7505_57	1999.1747	2000.0981	0.001	0.0454	-0.0059	0.0313	0.0042	0.0107	0.045	0.0317	f814w
wfpc2	7505_71	7505_77	1999.0815	2000.0942	0.013	0.0304	-0.0109	0.0362	-0.0001	0.0128	0.03	0.0364	f814w
wfpc2	7505_72	7505_77	1999.098	2000.0942	0.0546	0.0375	0.0152	0.0439	0.0002	0.0126	0.0374	0.0439	f814w
wfpc2	7505_74	7505_77	1999.1377	2000.0942	-0.0014	0.033	0.0066	0.0327	-0.0032	0.0125	0.0279	0.0331	f814w
wfpc2	8059_fq	9634_9k	2001.6381	2002.6175	1.6396	0.1912	0.3531	0.039	-0.002	0.0122	0.4827	0.0565	f606w
wfpc2	8090_of	8805_m0	1999.7202	2000.721	-0.0398	0.0504	0.0543	0.046	0.0119	0.0089	0.0497	0.0456	f606w
wfpc2	8090_og	8805_m0	1999.7204	2000.721	-0.0047	0.0446	0.0057	0.0492	0.006	0.0087	0.0442	0.049	f606w
wfpc2	8090_op	8805_m0	1999.7471	2000.721	-0.0216	0.053	-0.0281	0.0725	0.006	0.0115	0.067	0.0715	f606w
wfpc2	8090_oz	8805_m0	1999.7474	2000.721	0.0018	0.0456	0.0126	0.051	0.0185	0.0089	0.0434	0.0492	f606w
wfpc2	8490_01	9342_02	1999.4484	2001.4185	-0.0073	0.0139	0.023	0.0139	-0.0018	0.0096	0.0141	0.0139	f555w
wfpc2	8490_01	9342_02	1999.4482	2001.4185	-0.0077	0.0158	0.0261	0.0154	-0.0014	0.007	0.0158	0.0155	f814w
wfpc2	8654_02	9342_02	2001.4185	2003.396	-0.0194	0.0117	0.0221	0.0123	-0.0018	0.0114	0.0113	0.0113	f555w
wfpc2	8654_02	9342_02	2001.4185	2003.3961	-0.0186	0.0142	0.0234	0.0147	-0.0031	0.0071	0.0142	0.0145	f814w
wfpc2	8805_lz	8805_m0	2000.7208	2000.721	-0.0374	0.0423	0.0094	0.0428	0.0016	0.0089	0.0424	0.0428	f606w
wfpc2	8805_va	8805_vd	2001.1125	2001.113	0.4435	0.0471	-0.3174	0.0523	-0.0062	0.0095	0.0465	0.0526	f606w
wfpc2	8805_vb	8805_vd	2001.1126	2001.113	0.0003	0.0443	0.0012	0.0454	0.0008	0.0094	0.0444	0.0454	f606w
wfpc2	8805_vc	8805_vd	2001.1128	2001.113	1.3294	0.0469	0.5207	0.0475	-0.0031	0.0096	0.0469	0.0478	f606w
wfpc2	8805_xp	10084_fh	2001.1569	2004.1622	-0.0317	0.0329	-0.0131	0.0288	0.0012	0.0075	0.0329	0.0289	f606w
wfpc2	9244_cj	10084_fh	2001.3013	2004.1622	-0.0169	0.0266	-0.0095	0.0222	-0.0008	0.0076	0.0264	0.022	f606w
wfpc2	9244_q1	9244_q6	2001.7373	2001.7382	-0.9106	0.0389	-0.2308	0.0502	0.003	0.0104	0.0389	0.0502	f606w
wfpc2	9244_q2	9244_q6	2001.7375	2001.7382	-0.613	0.0373	0.0375	0.0493	-0.0016	0.0107	0.0373	0.0491	f606w
wfpc2	9244_q3	9244_q6	2001.7377	2001.7382	-1.0057	0.0412	-0.3443	0.0438	0.0009	0.0106	0.0414	0.044	f606w
wfpc2	9244_q4	9244_q6	2001.7378	2001.7382	-0.4757	0.0457	-0.0337	0.0493	0.0016	0.0105	0.0455	0.052	f606w
wfpc2	9244_q5	9244_q6	2001.738	2001.7382	-0.7291	0.0401	-0.5218	0.0459	0	0.0104	0.0402	0.0461	f606w
wfpc2	9244_s6	9709_xv	2001.7933	2003.9718	-0.0573	0.0241	-0.0129	0.0227	-0.0076	0.0085	0.0237	0.0217	f606w
wfpc2	9318_9x	10084_fh	2001.9931	2004.1622	0.0036	0.0273	-0.0216	0.0219	-0.001	0.0078	0.0267	0.0211	f606w
wfpc2	9318_dv	10084_de	2002.0551	2004.1159	0.0748	0.04	0.33	0.0401	-0.0052	0.0103	0.042	0.04	f606w
wfpc2	9318_e0	10084_de	2002.0602	2004.1159	0.0565	0.0529	0.3678	0.0461	-0.0077	0.0101	0.0521	0.0461	f606w
wfpc2	9318_e1	10084_de	2002.0603	2004.1159	0.0769	0.0557	0.2422	0.0425	-0.0084	0.0101	0.0546	0.0428	f606w
wfpc2	9634_9j	9634_9k	2002.6172	2002.6175	1.5515	1.7701	0.2875	0.047	0.0699	0.0105	5.9459	1.406	f606w
wfpc2	9676_g2	9710_vt	2002.719	2003.6395	0.3956	0.126	-0.0569	0.0645	-0.0087	0.0027	0.411	0.1206	f606w
wfpc2	9676_id	9709_r5	2002.7439	2003.7441	-0.0118	0.0323	0.0345	0.0378	-0.0101	0.0133	0.0366	0.0372	f606w
wfpc2	9676_je	9709_r5	2002.7565	2003.7441	0.0055	0.0348	0.1045	0.0305	-0.0058	0.0133	0.0374	0.0304	f606w
wfpc2	9676_qu	9709_r5	2003.7315	2003.7441	0.1137	0.0385	0.0649	0.0297	-0.0082	0.0118	0.0422	0.0298	f606w
wfpc2	9676_re	10084_fh	2002.9872	2004.1622	0.0027	0.0237	0.0015	0.0224	0.0011	0.0075	0.0238	0.0224	f606w
wfpc2	9676_w8	10084_fh	2003.1607	2004.1622	-0.0048	0.0253	-0.0107	0.0217	-0.0046	0.0074	0.0252	0.0213	f606w
wfpc2	9677_l2	9677_m0	2002.6098	2002.61	0.0131	0.0718	0.0091	0.0325	0.0011	0.0034	0.1186	0.0632	f300w
wfpc2	9677_l2	9677_m0	2002.6098	2002.61	0.0134	0.0739	0.0081	0.0326	0	0.0031	0.1235	0.0702	f606w
wfpc2	9677_l3	9677_m0	2002.6099	2002.61	-0.0249	0.0695	0.0011	0.0318	-0.0011	0.0033	0.1164	0.0573	f300w
wfpc2	9677_l3	9677_m0	2002.6099	2002.61	-0.0267	0.0722	0.0014	0.0334	-0.0005	0.0029	0.1272	0.0655	f606w
wfpc2	9677_tt	9710_vt	2002.7189	2003.6396	0.2212	0.0625	0.2317	0.025	-0.0029	0.0044	0.1457	0.0471	f300w
wfpc2	9677_tt	9710_vt	2002.7189	2003.6395	0.2356	0.131	0.2309	0.0433	-0.0033	0.0022	0.3797	0.1098	f606w
wfpc2	9709_a7	10084_fh	2003.2944	2004.1622	0.0128	0.0252	-0.0279	0.0204	0	0.0083	0.0252	0.0206	f606w
wfpc2	9709_nh	9710_vt	2003.6395	2003.6395	0.35	0.1227	-0.083	0.0375	-0.0073	0.0023	0.3541	0.1086	f606w

Table 2: Plate Scale and Both Skews

Data Sets Compared	Δ Plate Scale	Skew (Plate Scale)[a]	Skew (Axis)[a]
08048_02, 05941_04	X	$7.430 \pm 7.431 \times 10^{-5}$	$-7.737 \times 10^{-6} \pm 9.832 \times 10^{-5}$
08048_02, 07274_04	$11.14 \pm 7.993 \times 10^{-5}$	X	$2.774 \pm 9.063 \times 10^{-5}$

[a] Skew definitions can be found in Section 3.3.

3.4. Differential Magnitudes

From the paired source lists differential magnitudes were calculated by subtracting the magnitudes associated with each match. Outliers are defined as being more than 3σ away from the mean differential magnitude and were eliminated. All means quoted are calculated after the outliers have been discarded. The source lists contain magnitudes derived from $0.10''$ and $0.30''$ aperture photometry. Figures 9 and 10 plot the differential magnitudes against magnitudes. In the plots are the overall mean values of the differential magnitudes and are shown as solid horizontal black lines, whose values along with RMSs are presented in Table 3. The columns of Table 3 are data sets compared, dates when the observations were taken, $0.10''$ differential magnitudes and standard deviations, $0.30''$ differential magnitudes and standard deviations, and filters used in the observations. The means, RMSs, and median errors can be found in the legend in the upper left corner. The magnitudes are placed into bins: the first bin has a range of four magnitudes to help ensure that there are enough points to derive robust statistics, the second and third bins are each one magnitude wide, while the last bin is set to have a variable width based upon the faintest magnitude present in the source list. These bin widths are shown as the first two numbers in the legend. The next two numbers are the number of data points in the bins and the first number is the number of data points after a 3σ clipping, while the next number (in parenthesis) is the number of data points in the bin without 3σ clipping. The next two numbers are the means and RMSs in each particular bin. The last number is the median error in each magnitude bin. The vertical red bars are indicative of the median error in each magnitude bin. The small values of the overall mean shows that the aperture photometry is done properly and that SExtractor is producing reasonable fluxes for the $0.30''$ aperture. When comparing columns 6 and 8 it is clear that the mean differential magnitudes derived from the $0.30''$ aperture are consistently less than 0.1(6 cases > 0.1 out of 81; 7.40%), while for the mean differential magnitudes generated from the $0.10''$ aperture there are 22 cases out of 81 (27.2%) where the values are greater than 0.1. Moreover, DAOphot mean differential magnitudes (Wolfe & Castertano 2011b) for the $0.10''$ aperture are less than 0.1, except for 7 cases and note that the same paired source lists are used for the DAOphot and SExtractor source list examinations.

Furthermore, this also shows that the matching of the two source lists is done in a robust manner. Moreover, inspection of Figures 9 and 10 also reveals that the photometry is being produced correctly because the error and the scatter increase as objects become fainter. Note,

however, that the 0.10″ aperture photometry (top plot in Figures 9 and 10) has more scatter in the data, for bright as well as faint magnitudes, than for the 0.30″ aperture. This suggests that SExtractor, with it's present parameter configuration, is providing more robust calculations of the flux for the larger aperture.

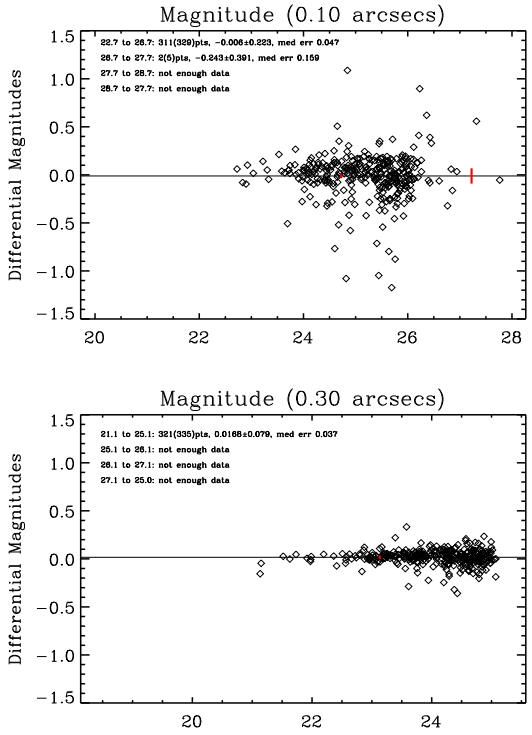

Fig. 9.— Shown in this figure are the differential magnitudes as a function of magnitude for 0.10″ and 0.30″ apertures. The solid line represents the mean differential magnitude. The source lists compared are 08048_02 and 05941_04.

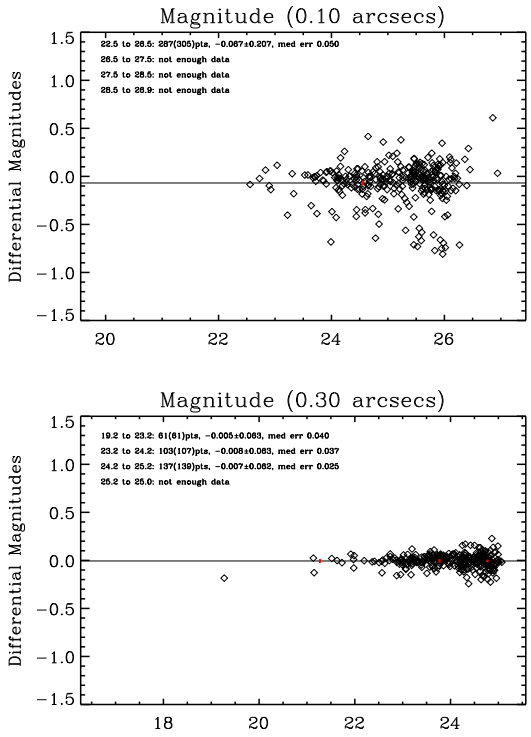

Fig. 10.— Shown in this figure are the differential magnitudes as a function of magnitude for 0.10″ and 0.30″ apertures. The solid line represents the mean differential magnitude. The source lists compared are 08048_02 and 07274_04.

Table 3: Mean Differential Magnitudes

Instr	Data Comp	Data Ref	Date Comp	Date Ref	0.10″ Aper.	0.10″ Stddev	0.30″ Aper.	0.30″ Stddev	Filter
acs	9438_01	9438_13	2003.0385	2004.0870	0.0102	0.0840	0.0076	0.0407	f814w
acs	9438_01	9438_03	2003.0385	2003.0570	-0.0044	0.1689	0.0314	0.0738	f814w
acs	9438_02	9438_13	2003.0409	2004.0870	0.0097	0.0846	0.0070	0.0438	f814w
acs	9438_02	9438_03	2003.0409	2003.0570	0.0138	0.1599	0.0304	0.0731	f814w
acs	9438_03	9438_13	2003.0570	2004.0870	-0.0126	0.1859	-0.0267	0.0648	f814w
acs	9438_04	9438_05	2003.0517	2004.0793	-0.0191	0.0903	-0.0120	0.0465	f555w
acs	9811_01	9811_05	2004.2129	2004.2961	-0.0099	0.0935	-0.0083	0.0523	f606w
acs	9811_04	9811_05	2004.2951	2004.2961	0.0300	0.0937	0.0105	0.0515	f606w
wfpc2	5477_0d	8048_02	1995.0879	2001.8732	0.0148	0.2666	0.0186	0.0894	f814w
wfpc2	5941_04	8048_02	1995.8881	2001.8732	-0.0113	0.2305	0.0163	0.0798	f814w
wfpc2	7274_04	8048_02	1998.1485	2001.8732	-0.0726	0.2225	-0.0051	0.0694	f814w
wfpc2	8059_dd	8059_dh	2000.6166	2000.6214	-0.2394	0.5037	-0.0874	0.2482	f606w
wfpc2	8059_df	8059_dh	2000.6159	2000.6166	-0.0985	0.4345	-0.0630	0.2065	f606w
wfpc2	6129_04	6129_05	1996.0479	1996.0644	0.0395	0.3849	0.0276	0.2043	f814w
wfpc2	6251_3u	7274_23	1995.5132	1999.4537	0.4263	0.5551	0.2783	0.4681	f814w
wfpc2	6251_3v	7274_23	1995.5134	1999.4537	0.2042	0.2729	0.0732	0.1058	f814w
wfpc2	6251_3w	8090_if	1995.5138	1999.4533	0.2010	0.1982	0.0534	0.0866	f606w
wfpc2	6251_3x	8090_if	1995.5140	1999.4533	0.2039	0.1897	0.0580	0.0907	f606w
wfpc2	6251_3z	7274_22	1995.5037	1999.4565	0.1148	0.3446	0.1074	0.2154	f814w
wfpc2	6251_40	7274_22	1995.5039	1999.4565	0.1365	0.3034	0.0966	0.2559	f814w
wfpc2	6251_41	7274_22	1995.5041	1999.4565	0.0832	0.3008	0.0696	0.1990	f814w
wfpc2	6254_aa	6254_ac	1996.1622	1996.1625	0.0568	0.2775	0.0519	0.2109	f814w
wfpc2	6254_ab	6254_ad	1996.1623	1996.1627	-0.0175	0.1507	0.0069	0.0794	f606w
wfpc2	6802_7b	6802_7e	1997.4200	1997.4377	0.0250	0.3673	0.0825	0.3506	f814w
wfpc2	6802_7c	7909_jk	1997.4202	1998.3711	0.0402	0.2119	-0.0030	0.1009	f606w
wfpc2	6938_06	7629_05	1998.4949	1999.4241	0.0714	0.1442	-0.0508	0.1031	f814w
wfpc2	7202_ry	7202_s1	1997.7348	1997.7354	0.0441	1.4419	-0.0255	0.7067	f450w
wfpc2	7202_rz	7202_s0	1997.7350	1997.7352	0.1526	0.7581	0.0740	0.3774	f814w
wfpc2	7505_22	7505_26	1998.1072	1999.0995	0.0712	0.1856	0.0184	0.1009	f814w
wfpc2	7505_23	7505_26	1998.1289	1999.0995	0.0942	0.1326	0.0178	0.0753	f814w
wfpc2	7505_24	7505_26	1998.1694	1999.0995	0.0648	0.1121	0.0195	0.0766	f814w
wfpc2	7505_25	7505_26	1998.2165	1999.0995	0.0795	0.1310	0.0282	0.0849	f814w
wfpc2	7505_51	7505_57	1999.0813	2000.0981	0.0637	0.1902	0.0328	0.0961	f814w
wfpc2	7505_52	7505_57	1999.0976	2000.0981	0.1131	0.2649	0.0318	0.1279	f814w
wfpc2	7505_53	7505_57	1999.1173	2000.0981	0.0586	0.2108	0.0180	0.0917	f814w
wfpc2	7505_54	7505_57	1999.1374	2000.0981	0.0984	0.2380	0.0316	0.0944	f814w
wfpc2	7505_55	7505_57	1999.1556	2000.0981	0.0958	0.1952	0.0263	0.0868	f814w
wfpc2	7505_56	7505_57	1999.1747	2000.0981	0.0733	0.2809	0.0243	0.0935	f814w
wfpc2	7505_71	7505_77	1999.0815	2000.0942	-0.0581	0.1599	-0.0024	0.0907	f814w
wfpc2	7505_72	7505_77	1999.0980	2000.0942	-0.0421	0.1665	0.0112	0.0867	f814w
wfpc2	7505_74	7505_77	1999.1377	2000.0942	-0.0349	0.1329	-0.0076	0.0870	f814w
wfpc2	8059_fq	9634_9k	2001.6381	2002.6175	-0.0817	0.1750	-0.0314	0.0781	f606w
wfpc2	8090_of	8805_m0	1999.7202	2000.7210	-0.0023	0.1789	-0.0074	0.0947	f606w
wfpc2	8090_og	8805_m0	1999.7204	2000.7210	-0.0115	0.1599	-0.0028	0.0962	f606w
wfpc2	8090_op	8805_m0	1999.7471	2000.7210	-0.0685	0.2667	-0.0327	0.1046	f606w
wfpc2	8090_oz	8805_m0	1999.7474	2000.7210	-0.0337	0.2057	-0.0037	0.1103	f606w
wfpc2	8490_01	9342_02	1999.4484	2003.3960	-0.7584	0.2007	-0.7347	0.1398	f555w
wfpc2	8490_01	9342_02	1999.4482	2003.3961	-0.7828	0.0926	-0.7374	0.0941	f814w
wfpc2	8654_02	9342_02	2001.4185	2003.3960	-0.0355	0.1729	-0.0216	0.1066	f555w
wfpc2	8654_02	9342_02	2001.4185	2003.3961	-0.0288	0.0964	-0.0017	0.0906	f814w
wfpc2	8805_lz	8805_m0	2000.7208	2000.7210	-0.0090	0.1661	-0.0023	0.0828	f606w
wfpc2	8805_va	8805_vd	2001.1125	2001.1130	0.0448	0.2028	0.0092	0.1160	f606w
wfpc2	8805_vb	8805_vd	2001.1126	2001.1130	0.0263	0.2151	-0.0117	0.1036	f606w
wfpc2	8805_vc	8805_vd	2001.1128	2001.1130	0.0164	0.2666	-0.0043	0.1094	f606w
wfpc2	8805_xp	10084_fh	2001.1569	2004.1622	-0.1567	0.5495	-0.0557	0.2029	f606w
wfpc2	9244_cj	10084_fh	2001.3013	2004.1622	-0.1048	0.3682	-0.0517	0.2013	f606w
wfpc2	9244_q1	9244_q6	2001.7373	2001.7382	0.0301	0.1904	0.0048	0.1047	f606w
wfpc2	9244_q2	9244_q6	2001.7375	2001.7382	0.0314	0.1722	-0.0014	0.0882	f606w
wfpc2	9244_q3	9244_q6	2001.7377	2001.7382	0.0104	0.1617	0.0035	0.0846	f606w
wfpc2	9244_q4	9244_q6	2001.7378	2001.7382	0.0347	0.2284	0.0080	0.0971	f606w
wfpc2	9244_q5	9244_q6	2001.7380	2001.7382	0.0069	0.1869	0.0022	0.0873	f606w
wfpc2	9244_s6	9709_xv	2001.7933	2003.9718	-0.1149	0.5391	-0.0407	0.2004	f606w
wfpc2	9318_9x	10084_fh	2001.9931	2004.1622	-0.1680	0.4310	-0.0249	0.1983	f606w
wfpc2	9318_dv	10084_de	2002.0551	2004.1159	0.0281	0.1873	0.0172	0.1264	f606w
wfpc2	9318_e0	10084_de	2002.0602	2004.1159	-0.0055	0.2633	0.0072	0.1374	f606w
wfpc2	9318_e1	10084_de	2002.0603	2004.1159	0.0185	0.2186	0.0259	0.1182	f606w
wfpc2	9634_9j	9634_9k	2002.6172	2002.6175	-0.1312	0.6569	-0.0487	0.4671	f606w
wfpc2	9676_g2	9710_vt	2002.7190	2003.6395	0.1793	1.4597	-0.0003	0.5391	f606w
wfpc2	9676_id	9709_r5	2002.7439	2003.7441	0.0889	0.1341	0.0230	0.0761	f606w
wfpc2	9676_je	9709_r5	2002.7565	2003.7441	0.0810	0.1366	0.0180	0.0685	f606w
wfpc2	9676_qu	9709_r5	2003.7315	2003.7441	0.0913	0.1286	0.0230	0.0740	f606w
wfpc2	9676_re	10084_fh	2002.9872	2004.1622	0.0294	0.2667	0.0030	0.1330	f606w
wfpc2	9676_w8	10084_fh	2003.1607	2004.1622	0.0576	0.2760	0.0235	0.1416	f606w
wfpc2	9677_l2	9677_m0	2002.6098	2002.6100	-0.0997	0.4591	-0.0056	0.2756	f300w
wfpc2	9677_l2	9677_m0	2002.6098	2002.6100	-0.3452	0.8246	-0.1778	0.2695	f606w
wfpc2	9677_l3	9677_m0	2002.6099	2002.6100	-0.0128	0.4011	0.0007	0.2815	f300w
wfpc2	9677_l3	9677_m0	2002.6099	2002.6100	-0.3164	0.8057	-0.1853	0.2946	f606w
wfpc2	9677_tt	9710_vt	2002.7189	2003.6396	0.1163	0.3273	-0.0422	0.2326	f300w
wfpc2	9677_tt	9710_vt	2002.7189	2003.6395	0.2623	1.2388	0.0660	0.4195	f606w
wfpc2	9709_a7	10084_fh	2003.2944	2004.1622	0.0489	0.3792	0.0508	0.1910	f606w
wfpc2	9709_nh	9710_vt	2003.6395	2003.6395	0.2750	1.0847	0.0419	0.3071	f606w

4. Part II: Overall Source List Comparison Results

4.1. Differential Astrometry

In this section we will explore the relationship between differential right ascension and differential declination as functions of each other and as a function of the date of the observations. In Figure 11 it is clear that most of the astrometric offsets are centered around zero with a range of $0.2''$. Both Guide Star Catalog I (GSC I; Russell et al. 1990) and Guide Star Catalog II (GSC II; Lasker et al. 2008) have 3σ values of $\approx 2.0''$ and $\approx 0.7''$, respectively. The larger offsets ($\geq 0.2''$ but $\leq 2.0''$) are reasonable because they fall within the 3σ of GSC I and GSC II. There is one outlier at a ΔRA $\approx$ 3.4967 and ΔDec $\approx$ -1.1875 and this outlier could be caused by poor registration of the astrometry with other database such as the Sloan Digital Sky Survey (SDSS; Pier et al. 2003), 2-Micron All Sky Survey (2MASS; Skrutskie et al. 2006), and GSC II during the multidrizzle process.

We examine a large offset that has been derived from the paired source lists 06254_ac and 06254_aa . The results can be found in Table 4 whose columns are: data sets compared in the first column, differential right ascension and differential declination in arcsecs and calculated with IDL in columns 2 and 3, while the last two columns are the same as 2 and 3 except for the offsets were calculated by hand using the right ascension and declination associated with each observation. It is readily apparent from the values in Table 4 that the calculations of the offsets from IDL and by hand are essentially the same. The small differences in the third and fourth decimal places can be attributed to differences in the precision in the right ascension and declination values derived from the HLA interface and the source lists derived from HLA. So it is not that these large offsets should be considered outliers, in the sense that there is an error but that the IDL software programs used are robust in deriving accurate astrometric offsets. Since there are no offsets that are greater than $10''$ and since the leeway in matching FOVs is $10''$ then this implies that robust astrometric offsets are being calculated.

Analysis of Figure 12 implies that there does not seem to be any correlation with time apparent in the data. In the top plot there does not seem to be any time difference dependence as all of the large offsets have time differences of 0 and 1, while for the smaller offsets the Δyear range is from 0 to $\approx$ 7 and are distributed around offsets of zero. The bottom plot shows essentially the same behavior except for the three larger differential declination at time differences greater than 2.5. There does not appear to be any correlation with the negative offsets for the rest of the data points and this implies that there is no dependence on the time differences.

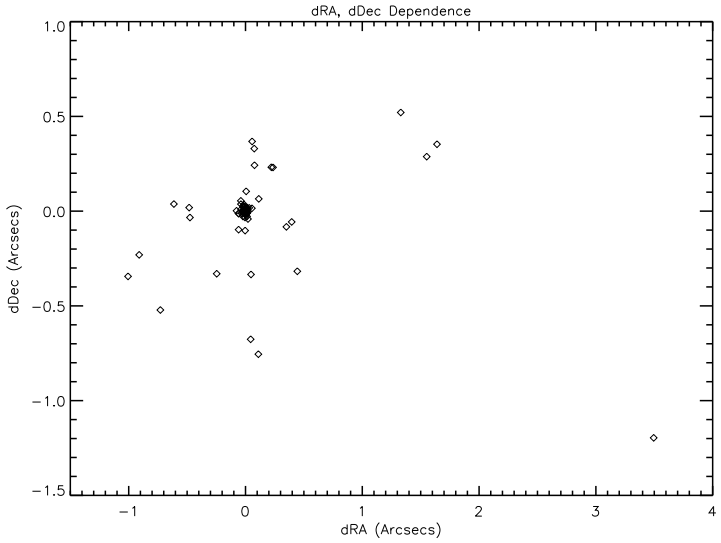

Fig. 11.— In this figure differential declination is plotted as a function of differential right ascension.

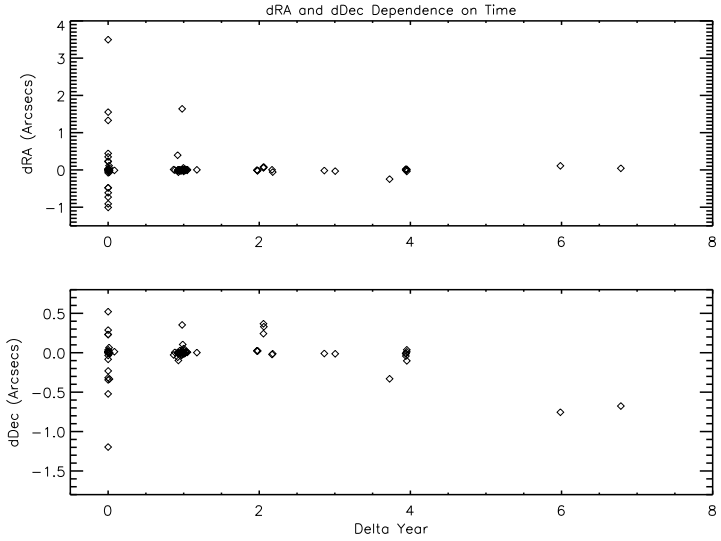

Fig. 12.— In this figure differential right ascension and differential declination are plotted as functions of Δyear. The Δyear values represent the differences in time of when the observations that went into generating two source lists were observed.

Table 4: Astrometric Offsets

Data Sets Compared	ΔRA (″, IDL)	ΔDec (″, IDL)	ΔRA (″, HLA)	ΔDec (″, HLA)
06254_ac, 06254_aa	3.495	-1.1964	3.495	-1.1800

4.2. Angles

As stated earlier rotational offsets were calculated and then removed from the source lists. All of the rotations derived from the paired source lists can be found in Figure 13 and plotted as a function of Δyear. As can be clearly seen there is a dichotomy in the distribution of angle values. The reason for this is that the observations span the period of WFPC2 history where two distinct focal plane solutions are used. The change to a different focal plane solution via a realignment of the Fine Guidance Sensor 1 (FGS1) resulted in the Science Instrument Aperture File (SIAF) being updated and this was on or about 1997.34. The large angles span a large enough time frame such that the compared source lists (not the reference source list) have observations dates that precede 1997.34 and the reference lists all have observation dates that occur after 1999.45. As a result the observations that generated the paired source lists have two different focal plane solutions and it could be that in the *idctab* reference file the information to correct for the two focal plane solutions was not propagated correctly. This has only been found in WFPC2 data so far. For the small angle measurements the dates of the compared source lists all have observation dates from 1996.05 to 1996.42 and 1997.42 to 2004.30. The reference source lists all have dates from 1996.06 to 1996.42 and 1997.44 to 2004.30. For the observations that created these paired source lists only one focal plane solution was used.

It can be inferred from Figure 13 that paired source lists that have a large Δyear value have large rotational offsets ($\geq 0.1''$). This, however, is an incorrect assumption. The reason for this is because all that needs to occur for a large rotational offset is for the observations to be taken with two different focal plane solutions. The boundary, as stated earlier, is 1997.34 and if observations are taken on either side of this boundary then there will be rotational offset that is $\geq 0.1''$. Note that the requirement of a large Δyear value as suggested by Figure 13 are not required because the only requirement is that both observations were taken on dates that cross the 1997.34 boundary.

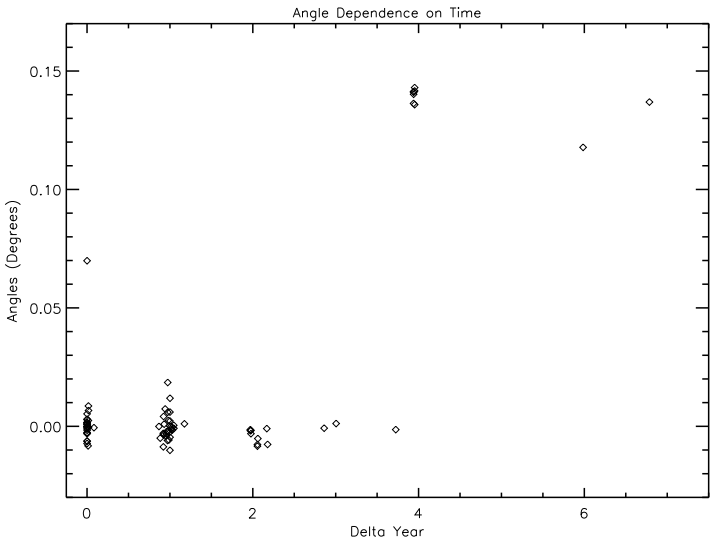

Fig. 13.— In this figure angles are plotted as functions of time differences. The abrupt increase in angle delineates the boundary in time where the solutions for the focal plane changed.

4.3. Differential Magnitudes

4.3.1. 0.30″ Aperture Magnitude

As opposed to the inspection of individual differential magnitudes, in this section all of the differential magnitudes are examined as a function of Δyear which is shown in Figures 14, 15, and 16 for the 0.30″ aperture magnitudes. All of the figures reveal a slope that can originate in sensitivity, throughput, qauntum efficiency (QE), and/or charge transfer efficiency (CTE) losses with time. However, CTE losses are the dominant source of signal loss (Gonzaga, private communication). This will result in calculated magnitudes being fainter for more recent exposures than for earlier observations as these exposures will be less affected by CTE losses. The positive slopes derived from the linear fits in Figures 14, 15, and 16 and the increasingly positive differential magnitude offsets do indeed imply that sensitivity, throughput, QE, and CTE losses have increased with time because in the paired source lists the reference source list is the more recent, while the compared source list is the earlier exposure. So when differential magnitudes are calculated the difference is taken as the reference magnitude subtracted from the compared magnitude resulting in a positive number that will increase in value as time progresses. This is because the reference magnitudes are increasingly affected by CTE losses, which make these reference magnitudes fainter as time evolves. Note that the magnitudes from the source lists have not been corrected for CTE losses. The slopes of the linear fits and the associated errors can be found in Table 5 for the 0.30″ apertures. Both tables have columns, which represent all filters, F606W, and F814W filters. The legend in the

top plots in all of the figures have the the linear equation describing the Δyear dependence of the differential magnitudes.

A test was done to see if WFPC2 CTE is consistent with the linear equations derived from the differential magnitudes as a function of Δyear. The most accurate photometry is from the $0.30''$ aperture and the largest Δyear is from data taken with the F814W filter. The linear equation from Figure 16 (see equation 1) was used as a check to see if CTE derived from the source list 8048_02 is consistent with the CTE calculated from the linear equation shown in Figure 16. The equation is presented for clarity:

$$\text{dmag} \quad = \quad 0.0080571718\text{x} - 0.0029192909 \tag{1}$$

where dmag is the differential magnitude, x is the Δyear and the slope has units of dmag/Δyear. Using a value of Δyear = 6.785302 the differential magnitude is 0.051751. Employing the WFPC2 CTE equations derived by Andrew Dolphin[3] and using a median flux value of $\approx 4134.72e^-$ from the source list 8048_02 and a background of $\approx 17e^-$ (derived from level 1 F814W data sets) the CTE in the y-direction is ≈ 0.078652. The differential magnitude of 0.051751 and the y-direction CTE of ≈ 0.078652 are consistent with each other suggesting that the slope of equation 1 is commensurate with the change in WFPC2 CTE as a function of time.

Another test was done to check the F606W filter of WFPC2. The linear equation tested in this case can be found in Figure 15 and is furnished in equation 2 for clarity:

$$\text{dmag} \quad = \quad 0.0044718477\text{x} - 0.0052173505 \tag{2}$$

where dmag is the differential magnitude, x is the Δyear and the slope has units of dmag/Δyear. Using a value of Δyear = 3.939576 the differential magnitude is 0.0123998. Employing the WFPC2 CTE equations from Dolphin and using a median flux value of $\approx 5378.80e^-$ from the source list 8090_if and a background of $\approx 10e^-$ (derived from level 1 F606W data sets) the CTE in the y-direction is ≈ 0.063068. The differential magnitude of 0.012340 and the y-direction CTE of ≈ 0.063068 are of the same order of magnitude suggesting that the slope of equation 2 gives an order of magnitude calculation when compared with the change in WFPC2 CTE as a function of time. Furthermore, when inspecting the differences between the CTE values derived from both procedures it is discovered that the differences are not the same *i.e.,* the F814W difference is 0.026901 and the F606W difference is 0.050688.

[3]http://purcell.as.arizona.edu/wfpc2_calib/2008_07_19.html

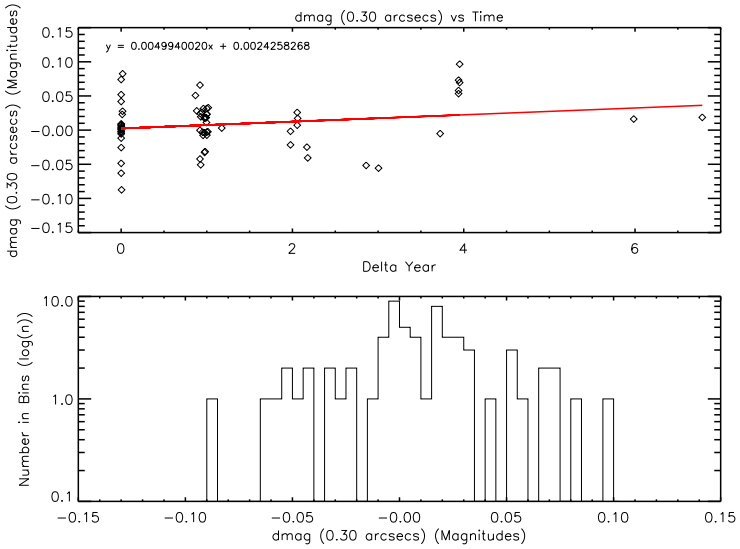

Fig. 14.— In this plot it is readily apparent that there is a time difference dependence on differential magnitudes, which can be seen in the top plot. The bottom plot is a histogram of the differential magnitudes. This plot includes all of the filters used in deriving the differential magnitudes at a 0.30″ aperture.

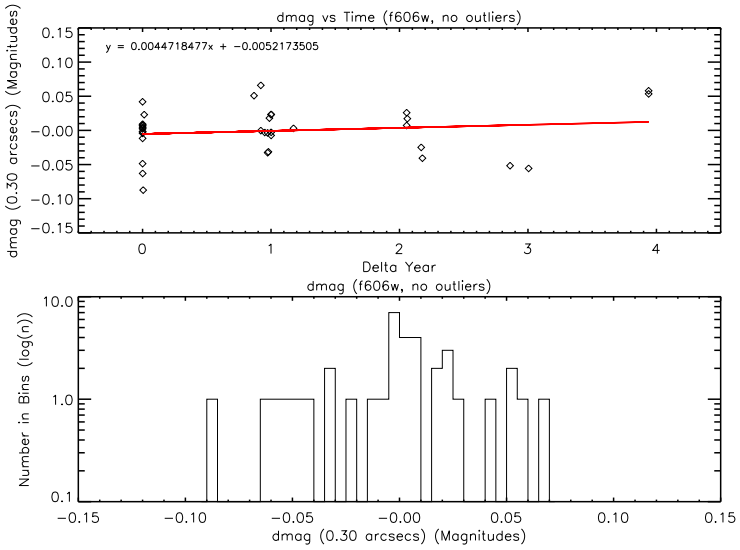

Fig. 15.— In this plot it is readily apparent that there is a time difference dependence on differential magnitudes, which can be seen in the top plot. The bottom plot is a histogram of the differential magnitudes. This plot includes only the F606W filter used in deriving the differential magnitudes at a 0.30″ aperture.

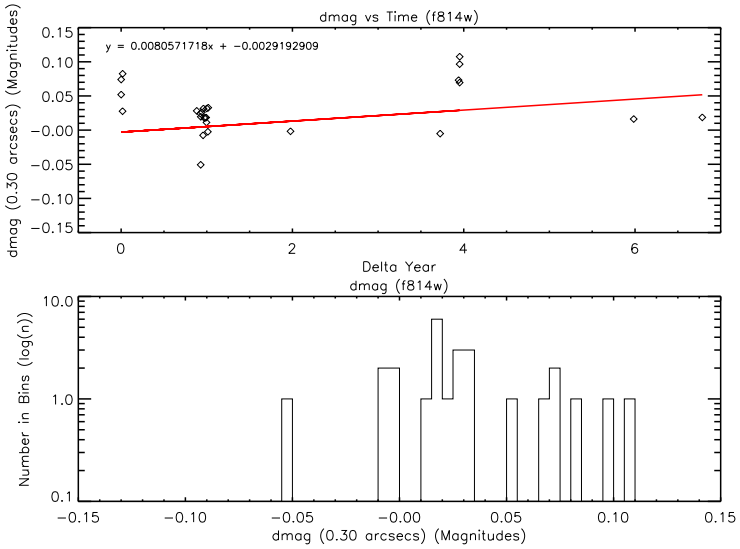

Fig. 16.— In this plot it is readily apparent that there is a time difference dependence on differential magnitudes, which can be seen in the top plot. The bottom plot is a histogram of the differential magnitudes. This plot includes only the F814W filter used in deriving the differential magnitudes at a 0.30″ aperture.

4.4. Outliers in Differential Magnitudes

Outliers have been defined as having mean values greater than or less than -0.1 and 0.1 differential magnitudes, respectively. Because SExtractor provides a more robust flux measurement for the 0.30″ aperture than for the 0.10″ aperture only the outliers for the 0.30″ aperture will be considered. Table 5 contains these large mean differential magnitude offsets and RMSs and the columns are: in the first column are the paired source lists, the second column is comprised of mean differential magnitudes, and the third column houses the filter used in the observation. Examination of the outliers will be done in sets based on the reference source lists, which are the first entries in column 1. Likewise, Figures 17, 18, 19, 20, and 21 will be used to help determine the voracity of the offsets in Table 6. Note that the legends in Figures 17, 18, 19, 20, and 21 all contain the same type of information namely: the instrument and filter incorporated, differential magnitude offset, proposal identifications and visit numbers of both the reference and compared source lists.

To start look at the first two sets of paired source lists with the reference file 7274_23 and 7274_22. Figures 17 and 18 reveal that these outliers have mean differential magnitudes greater than 0.1, however, in both cases (as is evidenced in the figures) there are numerous individual differential magnitude values that are biasing the mean differential magnitudes towards larger values. If these data points were excluded the mean differential would be ≈ 0.1 for 7274_23 and $\approx$ 0.05 for 7274_22. As a result the bias towards higher mean differential magnitude values is giving

false positives and these paired source lists are not in the outlier category.

The next paired source lists have the reference file 9342_02. As noted in Table 6 the 0.30″ aperture mean differential magnitude is ≈ -0.737 in the F814W filter. Analysis of Figure 19's top plot reveals that the distribution of data around the mean is fairly even giving credence to the value of the mean differential magnitude offset. Scrutiny Figure 19's bottom plot, a histogram, signifies that the peak of the distribution is ≈ -0.737. This outlier is found only in SExtractor derived source lists.

The penultimate set of paired source lists to explore have the reference file 9677_m0. As shown in Table 6 the mean differential magnitude is less than 0.1. Figure 20 has the plots of differential magnitudes and a histogram of the differential magnitudes. The top plot displays a distinct and odd shape for the distribution of data points and this therefore gives a robust measure of the mean differential offset of ≈ -0.122. Furthermore, the outlier nature is also manifested in the peculiar shape of the differential magnitude distribution. This same type of distribution can be found in the histogram of the bottom plot. The histogram clearly shows that a portion of the data is centered about 0, while other differential magnitudes range from ≈ -0.10 to -1.30.

The last set of paired source lists to explore have the reference file 9710_vt. As shown in Table 6 the mean differential magnitude is ≈ 0.042. Figure 21 has the plots of differential magnitudes and a histogram of the differential magnitudes. The top plot displays a distinct and odd shape for the distribution of data points and this therefore gives a robust measure of the mean differential offset. This same type of distribution can be found in the histogram of the bottom plot. The histogram clearly shows that a portion of the data is centered about 0, while other differential magnitudes range from ≈ -0.10 to -1.30.

Analysis of subsets of the data points using the IDL procedure aper.pro, which does aperture photometry, reveals approximately the same differential magnitude as the offsets implying that SExtractor is not the cause of the problem (Wolfe & Casertano 2011a).

Table 5: Outliers in Differential Magnitudes

Paired Source Lists	dmag 0.30″ Aper.	Filter
7274_23, 6251_3u	0.278 ± 0.468	F814W
7274_22, 6251_3z	0.107 ± 0.215	F814W
9342_02, 8490_01	-0.735[a]± 0.140	F555W
9342_02, 8490_01	-0.737[a]± 0.094	F814W
9677_m0, 9677_l2	-0.178 ± 0.270	F606W
9677_m0, 9677_l3	-0.185 ± 0.295	F606W
9710_vt,[b] 9709_nh[b]	0.042 ± 0.307	F606W

[a] This outlier was only found in SExtractor source lists.

[b] These particular data sets are designated an outlier because of the shape of the differential magnitude distribution is odd in magnitude space. See Figure 23.

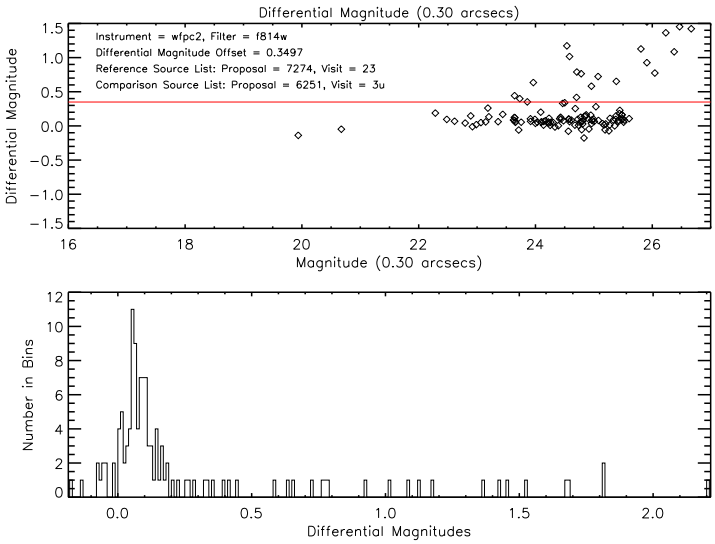

Fig. 17.— This is a plot of differential magnitudes with the mean overlaid as a red line shown in the top plot. The bottom plot shows a histogram of the differential magnitudes.

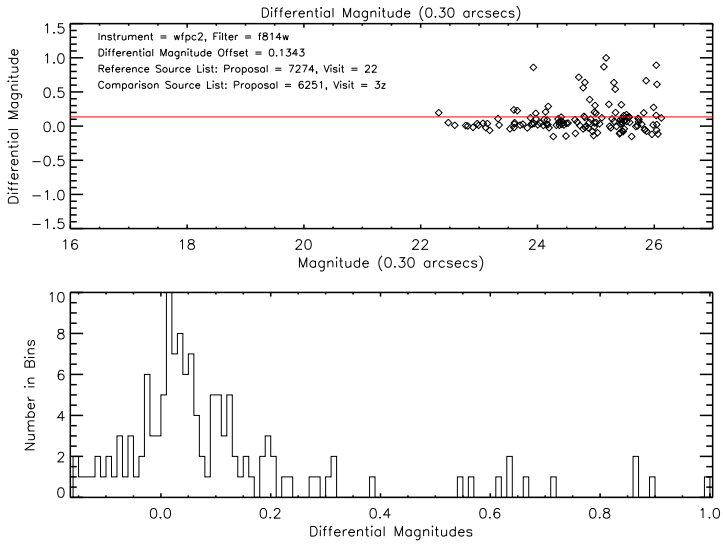

Fig. 18.— This is a plot of differential magnitudes with the mean overlaid as a red line shown in the top plot. The bottom plot shows a histogram of the differential magnitudes.

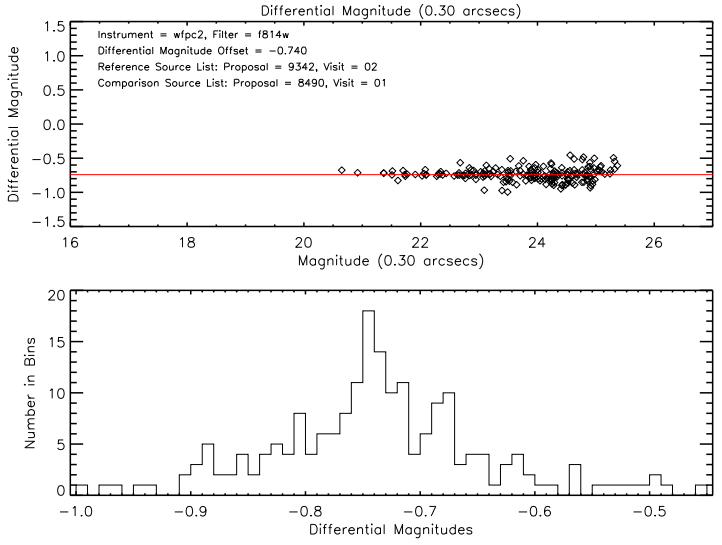

Fig. 19.— This is a plot of differential magnitudes with the mean overlaid as a red line shown in the top plot. The bottom plot shows a histogram of the differential magnitudes.

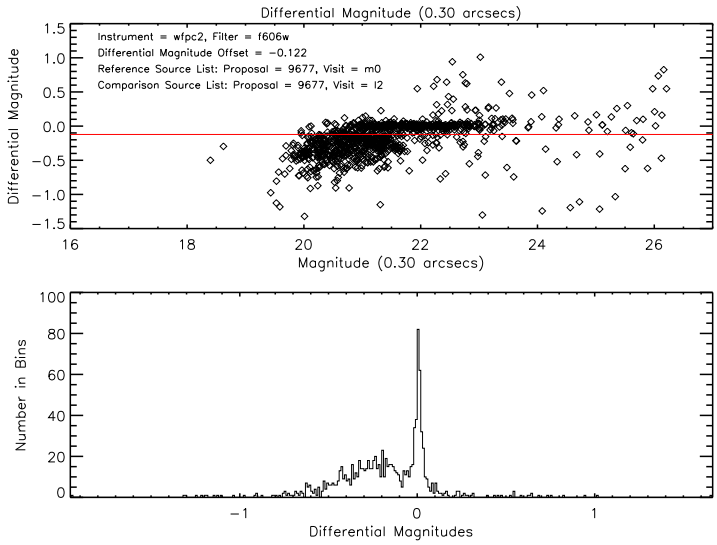

Fig. 20.— This is a plot of differential magnitudes with the mean overlaid as a red line shown in the top plot. The bottom plot shows a histogram of the differential magnitudes.

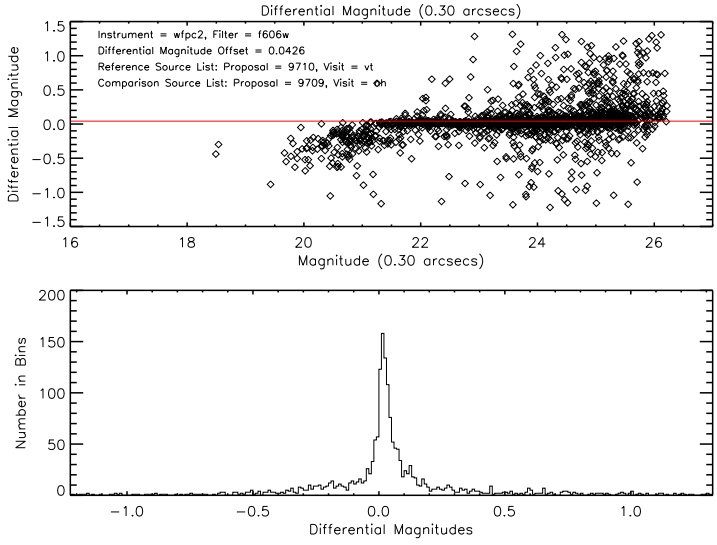

Fig. 21.— This is a plot of differential magnitudes with the mean overlaid as a red line shown in the top plot. The bottom plot shows a histogram of the differential magnitudes.

5. Conclusions

The examination of systematic properties of source lists as mentioned before is paramount when the product can be repeatedly used by a group of people. The preceding rigorous analysis supports the conclusion that the paired source lists are generated in a robust manner, although magnitudes are of a better quality for the $0.30''$ aperture than for the $0.10''$ aperture. The differential right ascension and differential declination show distinct distributions of data points that have large and small rotational offsets. Subsequently after the astrometric and rotational offsets have been eliminated the plots show random distributions centered around zero and have slopes associated with these distributions. This confirms that the algorithms employed to remove these offsets do this effectively. Because these offsets are removed efficaciously the result is that detector characteristics can be determined or at least estimated. Differential magnitudes communicate that the photometry is being accomplished robustly as well. The few outliers have been examined by reproducing the photometry, via an independent method, and have shown by calculating differential magnitudes that the problem does not lie with SExtractor, except for one case, but could instead be the result of anomalous observations.

Investigation of all of the paired source lists together divulges information pertaining to the overall quality inherent in the paired source lists. To begin it is important to note that the astrometric offsets did not exceed $10''$ as the leeway in pointings within the paired source lists is $10''$. Astrometric offsets were derived "by hand" using the right ascension and declination obtained through HLA and when compared to the values derived by our algorithms it was found that they are essentially the same. Interestingly enough, examination of the angles determined between paired source lists exemplifies that in using these analysis techniques it is possible to discover potential errors in reference files. It is also possible to see how CTE has caused magnitudes to decrease through interpretation of the dependence of differential magnitudes as a function of Δyear. As is readily apparent in the figures that demonstrate this dependence it is clear that for large time differences the differential magnitudes increase in value. Furthermore, CTE comparisons were made using Dolphin's CTE correction algorithms to derive CTE values and are consistent with the differential magnitudes values calculated from linear fits to differential magnitudes and Δyear. This implies that CTE, throughput, sensitivity, and QE losses (mainly CTE) are responsible for the differential magnitudes. Given that these losses are not taken into account in the generation of the $0.10''$ and $0.30''$ aperture magnitudes within the paired source lists it can be implied that the creation of the individual source lists is done in a consistent manner. Additional investigation needs to be done in order to achieve a full analysis of source lists generated not only by SExtractor but with DAOphot as well. Furthermore, since these analysis techniques are excellent in the investigation of detector characteristics it is therefore possible to discern relationships between the various instruments on HST and to map any changes that are revealed.

6. Acknowledgements

We would like to thank Jay Anderson for sharing his technique in determining astrometric offsets. We would also like to thank Rick White for sharing his idl procedures catmatch.pro and greatcircle.pro. We would also like to thank Shireen Gonzaga for her discussion of various WFPC2 topics.

7. References

Bertin, E. & Arnouts, S. 1996, A&AS, 117, 393

Kron, R. G., 1980, ApJS, 43, 305

Oke, J. B. & Gunn, J. E. 1983, ApJ, 266, 713

Pier, J. R., Munn, J. A., Hindsley, R. B., Hennessy, G. S., Kent, S. M., Lupton, R. H., & Ivezic, Z. 2003, AJ, 125, 1559

Skrutskie, M. F. et al., 2006, AJ, 131, 1163

Stetson, P. B. 1987, PASP, 99, 191

Wolfe, M. A., & Casertano, S., 2011a, HLA Document, "An Examination of the Large Mean Differential Magnitudes from Source Lists for WFPC2 and ACS Derived from DAOphot and SExtractor " (Baltimore: STScI)

Wolfe, M. A., & Casertano, S., 2011b, HLA Document, "An Examination of the Systematic Properties of Source Lists for WFPC2 and ACS Derived from DAOphot " (Baltimore: STScI)

8. Appendix

8.1. ΔPlate Scale (First Order Approximation)

This section shows mathematically how to derive to a first order approximation a change in the plate scale from two source lists that are separated in time. First start with the basic equations for x, y, x', and y':

$$x = x \tag{3}$$
$$y = y \tag{4}$$
$$x' = Sx \tag{5}$$
$$y' = Sy \tag{6}$$

where x and y are coordinates that are not scaled, whereas x', and y' are scaled quantities and S is the scaling factor. Now Δx and Δy are formulated in the following equations:

$$\Delta x = x' - x \tag{7}$$
$$= Sx - x \tag{8}$$
$$= x(S-1) \tag{9}$$

and

$$\Delta y = y' - x \tag{10}$$
$$= Sy - y \tag{11}$$
$$= y(S-1) \tag{12}$$

Now let:

$$x = \alpha \tag{13}$$
$$y = \delta \tag{14}$$
$$\Delta x = \Delta\alpha \tag{15}$$
$$\Delta y = \Delta\delta \tag{16}$$

where α is right ascension, $\Delta\alpha$ is the difference in right ascension from paired source lists, δ is the declination, and $\Delta\delta$ is the difference in declination between two source lists. Therefore equations 9 and 12 can be re-written using equations 13 through 16 as:

$$\Delta\alpha = \alpha(S-1) \tag{17}$$
$$\Delta\delta = \delta(S-1) \tag{18}$$

and rearranging:

$$\frac{\Delta\alpha}{\alpha} = (S-1) \tag{19}$$
$$\frac{\Delta\delta}{\delta} = (S-1) \tag{20}$$

Now to calculate the first order approximation of Δplate scale the average of the two slopes from plots of $\Delta\alpha$ vs. α and $\Delta\delta$ vs. δ are calculated. The equational form of this relationship can be found below:

$$\Delta\text{plate scale} = \frac{\frac{\Delta\alpha}{\alpha} + \frac{\Delta\delta}{\delta}}{2} \tag{21}$$

Equations 19 and 20 can be substituted into equation 21 to derive:

$$\begin{aligned} \Delta\text{plate scale} &= \frac{(S-1)+(S-1)}{2} && (22)\\ &= \frac{2(S-1)}{2} && (23)\\ &= S-1 && (24) \end{aligned}$$

It is interesting to note that Δplate scale can also be calculated from equations 19 and 20 assuming that the plate scale is the same for right ascension and declination. If the plate scale for right ascension and declination are different then this implies that:

$$S \neq S' \tag{25}$$

This further suggests that S' can be either the negative of S and/or some multiple of S or both at the same time. Equations 19 and 20 can then be written as:

$$\begin{aligned} \frac{\Delta\alpha}{\alpha} &= (S-1) && (26)\\ \frac{\Delta\delta}{\delta} &= (S'-1). && (27) \end{aligned}$$

A result of $S \neq S'$ is that the plate scale is not same for α and δ and this will introduce a skew between the α plate scale and the δ plate scale. The skew between plate scales is related through the difference in the plate scales:

$$\begin{aligned} \text{skew (plate scale)} &= \frac{\Delta\alpha}{\alpha} - \frac{\Delta\delta}{\delta} && (28)\\ &= (S-1)-(S'-1) && (29)\\ &= S-S' && (30) \end{aligned}$$

8.2. Rotation

This section derives how to calculate the rotation between paired source lists. First start with transformation equations:

$$\begin{aligned} x &= x && (31)\\ y &= y && (32)\\ x' &= x\cos\theta - y\sin\theta && (33)\\ y' &= x\sin\theta + y\cos\theta && (34) \end{aligned}$$

where x and y are coordinates that are not rotated, whereas x' and y' are rotated quantities with respect to x and y and $\cos\theta$ and $\sin\theta$ are the rotation factors, while θ is the angle between the paired source lists. Now Δx and Δy are formulated in the following equations:

$$\begin{aligned} \Delta x &= x' - x && (35)\\ &= x\cos\theta - y\sin\theta - x && (36)\\ &= x\cos\theta - x - y\sin\theta && (37)\\ &= x(\cos\theta - 1) - y\sin\theta && (38) \end{aligned}$$

and

$$\begin{aligned} \Delta y &= y' - y && (39)\\ &= x\sin\theta + y\cos\theta - y && (40)\\ &= x\sin\theta + y(\cos\theta - 1) && (41) \end{aligned}$$

now using the small angle approximation:

$$\begin{aligned} \cos\theta &\approx 1 && (42)\\ \sin\theta &\approx \theta. && (43) \end{aligned}$$

Substituting equations 42 and 43 into equations 38 and 41 thereby producing the following results:

$$\begin{aligned} \Delta x &\approx -y\theta && (44)\\ \Delta y &\approx x\theta && (45) \end{aligned}$$

and furthermore substituting equations 13 through 16 into equations 44 and 45 it is easy to see the dependence on right ascension and declination. The new equations are:

$$\begin{aligned} \Delta\alpha &\approx -\delta\theta && (46)\\ \Delta\delta &\approx \alpha\theta && (47) \end{aligned}$$

and rearranging to show the slope as a function of rotation angle

$$\begin{aligned} -\frac{\Delta\alpha}{\delta} &\approx \theta && (48)\\ \frac{\Delta\delta}{\alpha} &\approx \theta. && (49) \end{aligned}$$

Furthermore, if $\frac{\Delta\alpha}{\delta}$ and $\frac{\Delta\delta}{\alpha}$ have the same sign then a measure of the perpendicularity (another type of skew) between the right ascension and declination axes and can be found using the following equations:

$$\text{skew (non}-\text{perpendicularity)} = \frac{\frac{\Delta\alpha}{\delta} + \frac{\Delta\delta}{\alpha}}{2} \quad (50)$$

or

$$\text{skew (non}-\text{perpendicularity)} = \frac{-\frac{\Delta\alpha}{\delta} + -\frac{\Delta\delta}{\alpha}}{2} \quad (51)$$